

Original paper

Activation energy of annealed, partially metamict davidite by ^{57}Fe Mössbauer spectroscopy

Dariusz MALCZEWSKI^{1*}, Agnieszka GRABIAS², Maria DZIURWICZ¹¹ Institute of Earth Sciences, University of Silesia, Będzińska 60, 41-200 Sosnowiec, Poland; dariusz.malczewski@us.edu.pl² The Lukasiewicz Research Network – Institute of Electronic Materials Technology; Wólczyńska 133, 01-919 Warszawa, Poland

* Corresponding author



This study used ^{57}Fe Mössbauer spectroscopy to determine the activation energy for thermal recrystallization of partially metamict davidite [multiple oxide, $(\text{La,Ce,Ca,Th})(\text{Y,U})(\text{Ti,Fe}^{3+})_{20}\text{O}_{38}$]. Radioactive elements in metamict minerals damage crystal structure primarily due to recoil nuclei from α -decay of ^{238}U , ^{232}Th , ^{235}U , and their daughter products. Metamict minerals are widely used in geochronology and can serve as natural analogues for the study of radiation effects in high-level nuclear waste. Analysis was performed on fragments of a davidite sample collected from the Bektau-Ata alkaline granitoid massif (Kazakhstan). Electron-microprobe analysis showed that the sample may be classified as a davidite-(La) due to its La concentration of 3.14 wt. %, relatively low U of 0.88 wt. %, and Th of 0.25 wt. %. The calculated total absorbed α -dose was 8.1×10^{15} α -decay mg^{-1} . The concentration of Fe was 15 wt. % (2.1 % Fe^{2+} and 12.9 % Fe^{3+}). ^{57}Fe Mössbauer spectroscopy was carried out on fragments of the davidite sample after one-hour annealing under an argon atmosphere from 673 to 1373 K. A Fe^{2+} component was observed up to 1173 K. Variation in the ratio of amplitudes for the main absorption peaks in the Mössbauer spectra vs. annealing temperature appeared to be a sensitive indicator of thermally-induced recrystallization. The activation energy, $E_A = 0.45$ eV, for recrystallization was determined based on the exponential dependence of the amplitudes' ratio upon temperature and using an Arrhenius plot.

Keywords: partially metamict davidite, activation energy, Mössbauer spectroscopy, annealing

Received: 12 December 2019; **accepted:** 5 March 2020; **handling editor:** J. Plášil

1. Introduction

Davidite (multiple oxide) is a Fe–Ti–U-bearing mineral that is often metamict. It is generally associated with sodium-rich, acidic igneous rocks, pegmatites, granulite-facies metamorphic rocks, and hydrothermal veins (Whittle 1959; Neumann and Sverdrup 1960; Branagan 2007; Lumpkin et al. 2014; Singh et al. 2018). Davidite, $(\text{La, Ce, Ca, Th})(\text{Y, U})(\text{Fe, Mg})_2(\text{Ti, Fe, Cr, V})_{18}(\text{O, OH, F})_{38}$, is isostructural with crichtonite group minerals and crystallizes in the $R3$ space group (Pabst 1961; Rouse and Peacor 1968; Wülser et al. 2004). According to the prevailing element in the cation sites, it occurs in three forms – as davidite-(La), davidite-(Ce) and davidite-(Y) (Orlandi et al. 2004).

A polyhedral representation of crichtonite-group minerals shows that REEs occupy a large $^{XII}M(\text{O})$ site, whereas yttrium, uranium, and REE having smaller ionic radii occupy an octahedral $M(1)$ site (Gatehouse et al. 1979 and references therein). According to that representation the remaining small cations, mainly titanium and iron, occupy three other octahedral sites $M(3)$, $M(4)$, and $M(5)$, as well as the tetrahedral $M(2)$ site. The crichtonite-type structure was also proposed as a possible host phase for actinides and fission products in nuclear waste deposits (Lumpkin et al. 2014 and reference therein). Due to its

relatively high uranium and subordinate thorium contents, natural davidite specimens are mainly found in metamict (amorphous) state. Lumpkin et al. (2013) used electron diffraction methods to estimate a critical amorphization dose for 275–295 Ma davidites of about 0.8×10^{16} α -decay mg^{-1} . The temperature at which fully metamict davidite can recrystallize varies only slightly for samples collected from different geological environments. Research by Lima de Faria (1956) and Pabst (1961) showed that fully metamict davidites recrystallized at temperatures between 900 and 1000 °C for one-hour annealing time under atmospheric air. Further increase in annealing time (up to 24 h) and higher temperatures (up to 1375 °C) did not lead to significant changes in sample X-ray diffraction patterns (Lima de Faria 1956; Neumann and Sverdrup 1960; Pabst 1961; Gatehouse et al. 1979; Singh et al. 2018).

At present, there are only limited data on activation energies for recrystallization processes in metamict minerals. Table 1 lists previously reported values obtained using different methods. The aim of the current study was to determine the activation energy for thermally-induced recrystallization of partially metamict davidite using ^{57}Fe Mössbauer spectroscopy. The analysis also sought to record changes in hyperfine parameters of Fe^{2+} and Fe^{3+} components associated with the annealing processes.

Tab. 1 Previously reported activation energies for annealed metamict samples

Reference	Mineral	Activation energy (eV)	Methods
Saini et al. (1975)	Allanite	2.3 (range from 1.4–3.4)	Fission-track annealing
Virk (1995)	Zircon	2.87 (average from: 2.15, 2.87, and 3.60)	Fission-track annealing
Janeczek and Eby (1993)	Gadolinite (partially metamict)	0.58	X-ray diffraction
Meldrum et al. (1997)	Monazite	0.08	Irradiation by 800 keV Kr ²⁺
Malczewski and Janeczek (2002)	Gadolinite (fully metamict)	1.97	Mössbauer spectroscopy

2. Materials and methods

2.1. Sample description and chemical analysis

The davidite investigated here is a massive grayish black with vitreous–metallic luster. It was collected in granite pegmatite from Permian Bektau-Ata granitoid massif, Kazakhstan (Fig. 1a). After splitting the sample into fragments (Fig. 1b), the pieces were placed in quartz tubes, sealed under argon, and annealed for one hour in a muffle

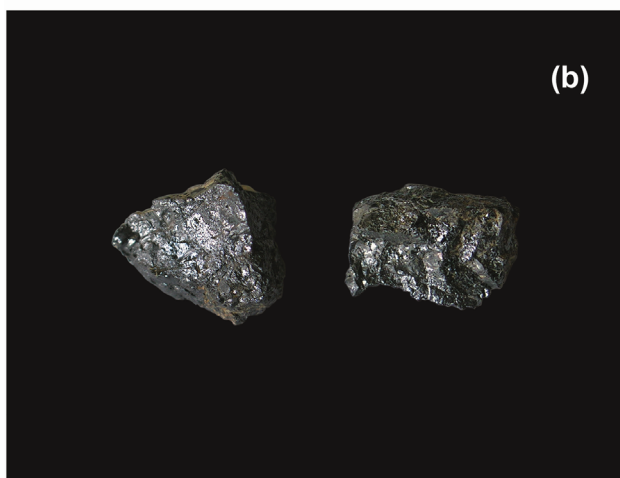


Fig. 1a – Photo of the original davidite specimen from Bektau-Ata (Kazakhstan), 4.5 cm in length. **b** – Internal fragments of the specimen analyzed in this study, ~1 cm in length.

furnace at 673, 873, 1073, 1173, 1273, and 1373 K. Each temperature was stabilized at ± 2 K. After annealing, the samples were quenched and ground into powder.

The composition of the sample was determined using a JEOL JSM-6480 scanning electron microscope at the Institute of Materials Engineering (University of Silesia) with an energy-dispersive X-ray spectrometer (SEM–

Tab. 2 Age, chemical composition (wt. %), ²²²Rn and ²²⁰Rn emanation coefficients, and calculated α -doses for the davidite sample examined in this study. Measurement uncertainties (1σ) are given in parentheses

Age	275(24) Ma ^a
O	29.2(14)
F	1.11(13)
Al	0.47(5)
Si	0.5(1)
Ca	0.26(6)
Ti	35.1(8)
Fe	14.6(5)
Ge	0.26(3)
Se	0.52(6)
Y	3.04(10)
Nb	0.88(15)
La	3.14(9)
Ce	2.4(1)
Dy	1.12(18)
Er	0.52(12)
Lu	0.43(3)
Ta	0.84(7)
W	0.89(3)
Pb	2.19(6)
Th	0.25(1)
U	0.83(3)
Total	99.90
Calculated total dose (D_T) ^b (α -decay mg ⁻¹)	$8.1(8) \times 10^{15}$
Calculated dose from ²³⁸ U (D_{238}) (α -decay mg ⁻¹)	7.2×10^{14}
Calculated dose from ²³⁵ U (D_{235}) (α -decay mg ⁻¹)	0.33×10^{12}
Calculated dose from ²³² Th (D_{232}) (α -decay mg ⁻¹)	0.53×10^{15}
e_{222} ^c	1.5×10^{-4} %
e_{220}	2.9×10^{-2} %

^a Permian age

^b Doses were calculated as: $D_{238} = 8 \times N_{238}(e^{\lambda_{238}t} - 1)$, $D_{235} = 7 \times N_{235}(e^{\lambda_{235}t} - 1)$, $D_{232} = 6 \times N_{232}(e^{\lambda_{232}t} - 1)$ and $D_T = D_{238} + D_{235} + D_{232}$. N_{238} , N_{235} and N_{232} are the present numbers of atoms of ²³⁸U, ²³⁵U and ²³²Th per milligram, λ_{238} , λ_{235} and λ_{232} are the decay constants of ²³⁸U, ²³⁵U and ²³²Th (respectively), and t is the geologic age. The absorbed ²³⁵U α -doses were calculated assuming a natural atomic abundance of ²³⁸U/²³⁵U = 137.88

^c ²²²Rn emanation coefficient (e_{222}) and ²²⁰Rn emanation coefficient (e_{220})

EDS) operated at an accelerating voltage of 20 kV and a beam current of 30 μ A. Data were analyzed using the EDS2006 software. The electron-microprobe data were obtained from three grains (collected from 39 points, in total) of the inner fragments of the specimen. The concentrations of ^{232}Th , ^{238}U , and ^{235}U were calculated based on gamma-ray activities of ^{228}Ac (^{232}Th), ^{226}Ra , ^{214}Pb , ^{214}Bi (^{238}U), and assuming a natural atomic abundance of $^{238}\text{U}/^{235}\text{U} = 137.88$. Gamma-ray spectra were collected at the Laboratory of Natural Radioactivity (University of Silesia) using a GX3020 HPGe detector (32% efficiency with energy resolution of 0.8 keV at 122 keV) and analyzed using Genie 2000 v.4 software. Table 2 lists chemical composition, calculated α -doses, and radon and thoron emanation coefficients.

2.2. Mössbauer spectroscopy and X-ray diffraction

For ^{57}Fe Mössbauer spectroscopy the powder fragments were prepared as a thin disc absorber. Mössbauer transmission spectra of the untreated fragment and annealed fragments were recorded at the Institute of Electronic Materials Technology (Warsaw) at room temperature using a constant acceleration spectrometer, a multichannel analyzer with 512 channels and linear arrangement of $^{57}\text{Co}/\text{Rh}$ source (= 50 mCi) absorber and detector. Mössbauer spectra were numerically analyzed using Recoil and MEP fitting software.

The untreated and annealed fragments were analyzed for their powder X-ray diffraction (XRD) patterns at the Institute of Physics (University of Silesia) using a SIEMENS D5000 diffractometer in the θ - θ geometry and CuK_α radiation in the scan mode with a step size of 0.02° and a counting time of 5 s at each step.

3. Results and discussion

3.1. Mössbauer spectroscopy of annealed fragments

The ^{57}Fe Mössbauer spectra and corresponding XRD patterns of davidite samples are shown in Fig. 2 (untreated sample) and Fig. 3 as a function of annealing temperature. The hyperfine parameters derived from the fitting procedure for each annealed sample are summarized in Tab. 3. The Mössbauer spectrum of the untreated davidite sample from Bektau-Ata is characterized by the presence of three quadrupole doublets assigned to Fe^{2+} (no. 1) and Fe^{3+} (no. 2 and 3) in $M(3)$ octahedral positions (Fig. 2a) (Hawthorne 1988). The larger Fe^{3+} (no. 3) doublet indicates these octahedra that have undergone a distortion relative to those observed in the davidite crystal matrix.

The powder XRD pattern (Fig. 2b) shows that the untreated sample is partially metamict despite an absorbed α -dose of 8.1×10^{15} α -decay mg^{-1} . Hence, in contrast to results reported by Lumpkin et al. (2013) suggesting that the amorphization dose for 275–295 Ma davidites is about 8×10^{15} α -decay mg^{-1} , our results suggest that the davidite amorphization dose exceeds 10^{17} α -decay mg^{-1} . This result resembles values calculated for other metamict phases having multiple oxides (Malczewski and Dziurawicz 2015).

The Mössbauer spectra can be fitted to three quadrupole doublets up to 1173 K (Fig. 3a–d). The Fe^{2+} component is absent in spectra of fragments annealed at 1273 and 1373 K (Fig. 3e–f) and the spectra can be fitted by one Fe^{3+} doublet unambiguously assigned to an octahedral position. There was no observed Fe^{3+} in tetrahedral $M(2)$ sites. This observation indicates that in crystalline phase of davidite from Bektau-Ata iron occurs only in the third oxidation state. The presence of Fe^{2+} in

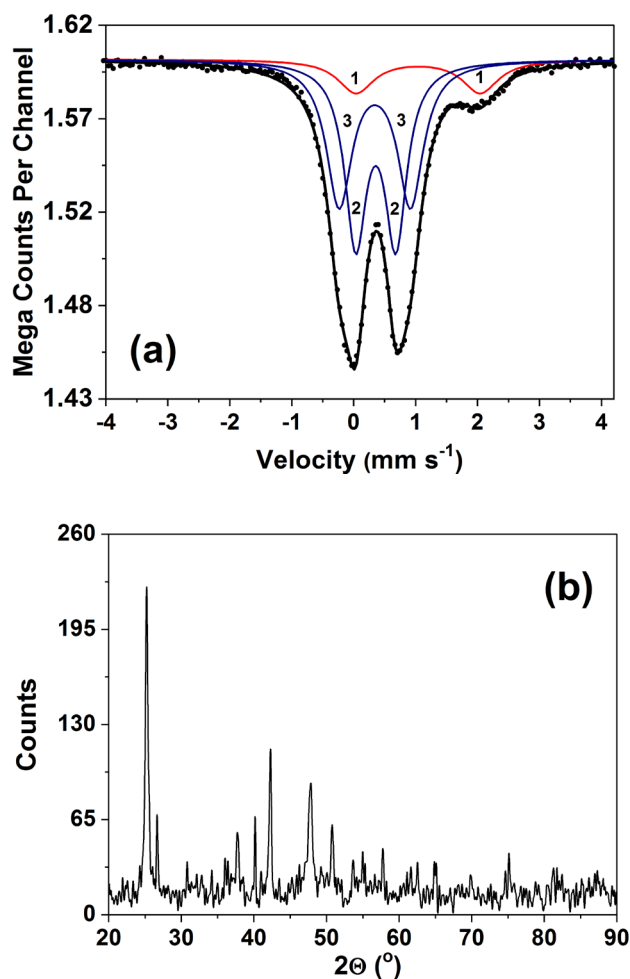
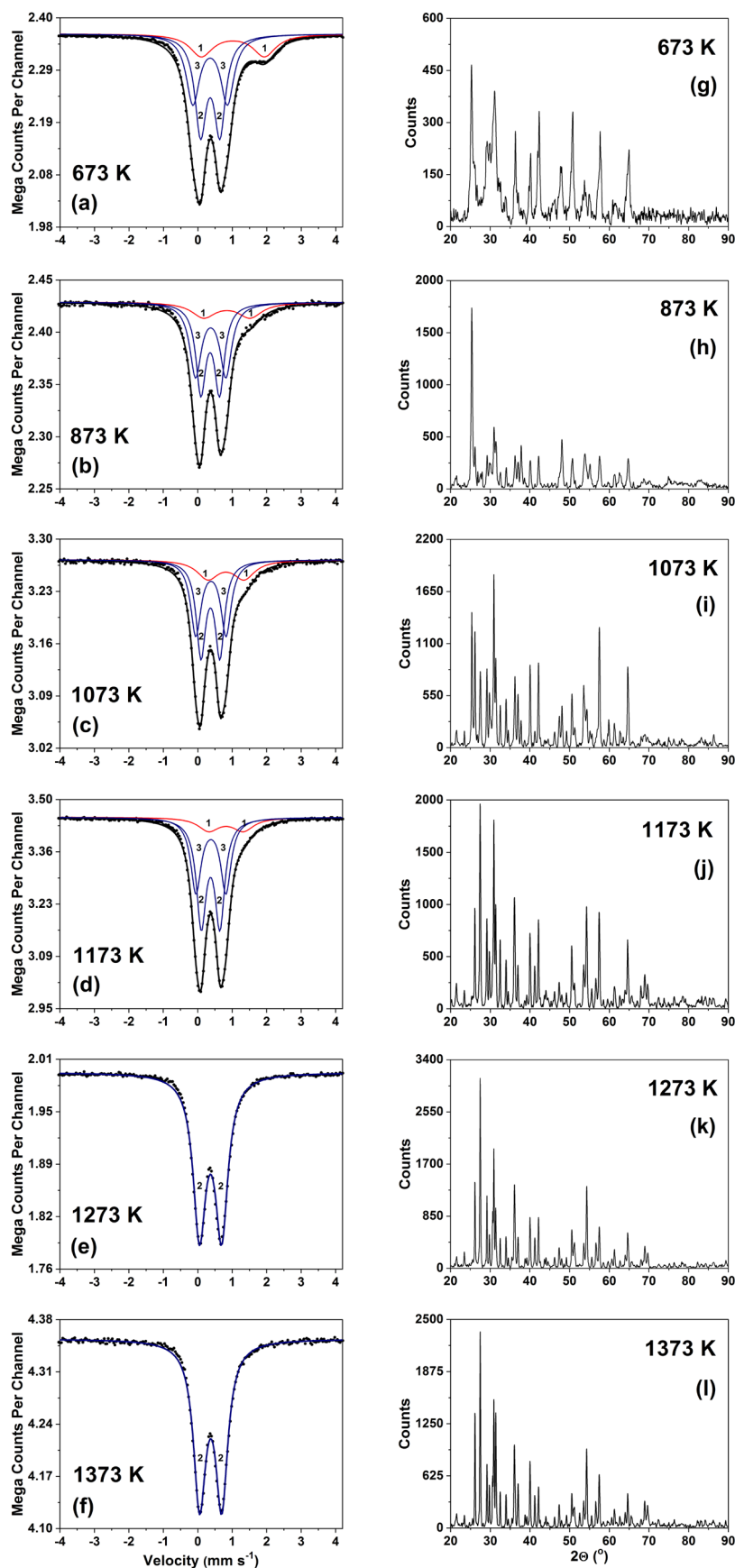


Fig. 2a – ^{57}Fe Mössbauer spectrum of untreated davidite sample. Solid dots = experimental data, thick solid line = fitted curve, thin solid line = fitted doublets. b – Corresponding XRD pattern.



partially metamict davidite presumably results from reduction of Fe^{3+} to Fe^{2+} in damaged regions of the mineral affected by metamictization. These aperiodic domains can incorporate a large amount of hydrogen (as OH^-) as a result of post-damage diffusion of H_2 into the structure (Hawthorne et al. 1991). Conversely, recrystallization can be accompanied by dehydroxylation with simultaneous Fe^{2+} to Fe^{3+} oxidation. Both IS (isomer shift) and QS (quadrupole splitting) values for the Fe^{2+} doublet decrease considerably with increasing annealing temperature (Tab. 3). This suggests a highly distorted geometry for the coordinated octahedra or a lowering of the coordination number. Changes of hyperfine parameters observed in the Mössbauer spectra coincide with XRD patterns (Figs. 3g–h). As shown in Fig. 3, the crystallinity of the annealed fragments increases with increasing temperature. Annealing at 1273 and 1373 K leads to a fully crystalline structure. These results are in line with those previously reported for annealed fully metamict davidites where recrystallization occurred between 900 °C (1173 K) and 1000 °C (1273 K). However, the annealing path of partially metamict davidite observed by Mössbauer spectroscopy differs significantly from paths obtained for fully metamict silicates (Malczewski 2010; Malczewski et al. 2018).

3.2. Determination of activation energy

Given a polyhedral geometry, metamictization process causes deformation and displacement of structural polyhedra. Thermal recrystallization restores the structural units to their normal positions as well as reestablishes distances and angles in cation polyhedra observed in the crystalline form

Fig. 3a–f – ^{57}Fe Mössbauer spectra acquired at room temperature of davidite fragments annealed in argon for 1 h at the given annealing temperatures T_A . Solid dots = experimental data, thick solid line = fitted curve, thin solid line = fitted doublets. **g–l** – Corresponding XRD patterns.

of the mineral. In this sense, activation energy for thermally-induced recrystallization of metamict minerals means the minimum energy required to restore structural polyhedra to their normal positions. This can consequently regenerate the original long-range order.

To determine the activation energy of partially metamict davidite, we propose an empirical isochronal annealing model based on modified models for annealing of fission fragment tracks in solids (Modgil and Virk 1985), and isothermal annealing and tempering (Primak 1955, 1960; Malczewski and Molak 2011). According to this model, the activation energy is essentially independent of temperature and annealing time but may depend on the degree of metamictization and annealing atmosphere (Malczewski 2010). We also assume that various metamict minerals can be characterized by different recrystallization temperatures (Seydoux-Gillaume et al. 2002; Zietlow et al. 2017). This temperature may be understood as the lowest temperature at which recrystallization must occur almost immediately. A quantity Q or the quantity change is usually assumed to represent the recrystallization rate that satisfies the Arrhenius expression in a general form:

$$Q(T) = A \exp\left(\left(-\frac{1}{T}\right)\frac{E_A}{k}\right) \quad (1)$$

where A is the proportional constant, E_A is the activation energy (eV), T the absolute temperature (K) and k is the Boltzmann's constant. Equation (1) can be expressed including recrystallization temperature T_R (K) as:

$$Q(T) = Q_R \exp\left(\left(\frac{1}{T_R} - \frac{1}{T}\right)\frac{E_A}{k}\right) \quad (2)$$

where Q_R is the value of Q at T_R .

As seen in Fig. 3 and Fig. 4a, amplitudes for the main absorption peaks in the Mössbauer spectra change significantly with annealing temperature relative to each other. This allows for selection of the parameter R that represents the ratio of amplitudes of high-energy to low-energy as an input for determining the activation energy of recrystallization as it occurs in partially metamict

Tab. 3 Parameters for ^{57}Fe Mössbauer spectra of annealed davidite samples (Figs 2 and 3). Isomer shift values (IS) are given relative to the $\alpha\text{-Fe}$ standard

T (K)	Doublet no.	χ^2	IS (mm s ⁻¹)	QS ^a (mm s ⁻¹)	$\Gamma/2^b$ (mm s ⁻¹)	Site (CN) ^c	Intensity
RT							
	1	1.6	1.04(3)	2.01(3)	0.35(2)	Fe ²⁺ (6)	0.14(1)
	2		0.36(1)	0.65(1)	0.21(1)	Fe ³⁺ (6)	0.44(2)
	3		0.34(1)	1.15(3)	0.25(1)	Fe ³⁺ (6)	0.42(2)
673							
	1	2.5	1.02(2)	1.83(2)	0.40(2)	Fe ²⁺ (6)	0.20(1)
	2		0.36(1)	0.56(1)	0.20(1)	Fe ³⁺ (6)	0.43(3)
	3		0.35(1)	1.00(1)	0.23(1)	Fe ³⁺ (6)	0.37(3)
873							
	1	1.4	0.85(2)	1.34(3)	0.42(3)	Fe ²⁺ (6)	0.17(3)
	2		0.36(1)	0.54(2)	0.18(1)	Fe ³⁺ (6)	0.42(3)
	3		0.38(1)	0.88(3)	0.20(1)	Fe ³⁺ (6)	0.41(3)
1073							
	1	1.7	0.82(2)	1.05(3)	0.38(3)	Fe ²⁺ (6)	0.19(3)
	2		0.37(1)	0.55(2)	0.18(1)	Fe ³⁺ (6)	0.43(3)
	3		0.38(1)	0.88(3)	0.18(1)	Fe ³⁺ (6)	0.38(3)
1173							
	1	2.2	0.82(2)	1.00(2)	0.37(3)	Fe ²⁺ (6)	0.13(1)
	2		0.37(1)	0.54(1)	0.17(1)	Fe ³⁺ (6)	0.49(3)
	3		0.38(1)	0.87(1)	0.18(1)	Fe ³⁺ (6)	0.38(3)
1273							
	2	1.7	0.37(1)	0.64(1)	0.22(1)	Fe ³⁺ (6)	1
1373							
	2	1.5	0.37(1)	0.64(1)	0.22(1)	Fe ³⁺ (6)	1

^a Quadrupole splitting, ^b half-width, ^c coordination number

davidite and determined from Mössbauer spectroscopic data. Figure 4b shows variation in R with temperature. As seen in Fig. 4, progressive recrystallization between 673 and 1273 K in argon is characterized by a single-stage mechanism wherein R equals unity at 1273 K and does not increase after annealing at 1373 K (Fig. 3f).

The rate of change in the amplitudes' ratio to temperature, $\partial R/\partial T$, is a well-defined exponential function with respect to the inverse temperature ($1/T$) and meets the requirements of the proposed isochronal annealing model (Eq. 2). This derivative function shown in Fig. 5a can be described as:

$$\frac{\partial R}{\partial T} = \left(\frac{\partial R}{\partial T}\right)_R \exp\left(\left(\frac{1}{T_R} - \frac{1}{T}\right)\frac{E_A}{k}\right) \quad (3)$$

where $(\partial R/\partial T)_R$ refers to the value of the derivative at $T_R = 1273$ K.

The logarithm of the function given by Eq. (3) (Fig. 5b) plotted against the inverse temperature forms a straight line:

$$\ln\left(\frac{\partial R}{\partial T}\right) = b - \frac{1}{T}a \quad (4)$$

with slope $a = 5258(230)$ and intercept $b = -3.849(1)$. Since $a = E_A/k$, the calculated activation energy is:

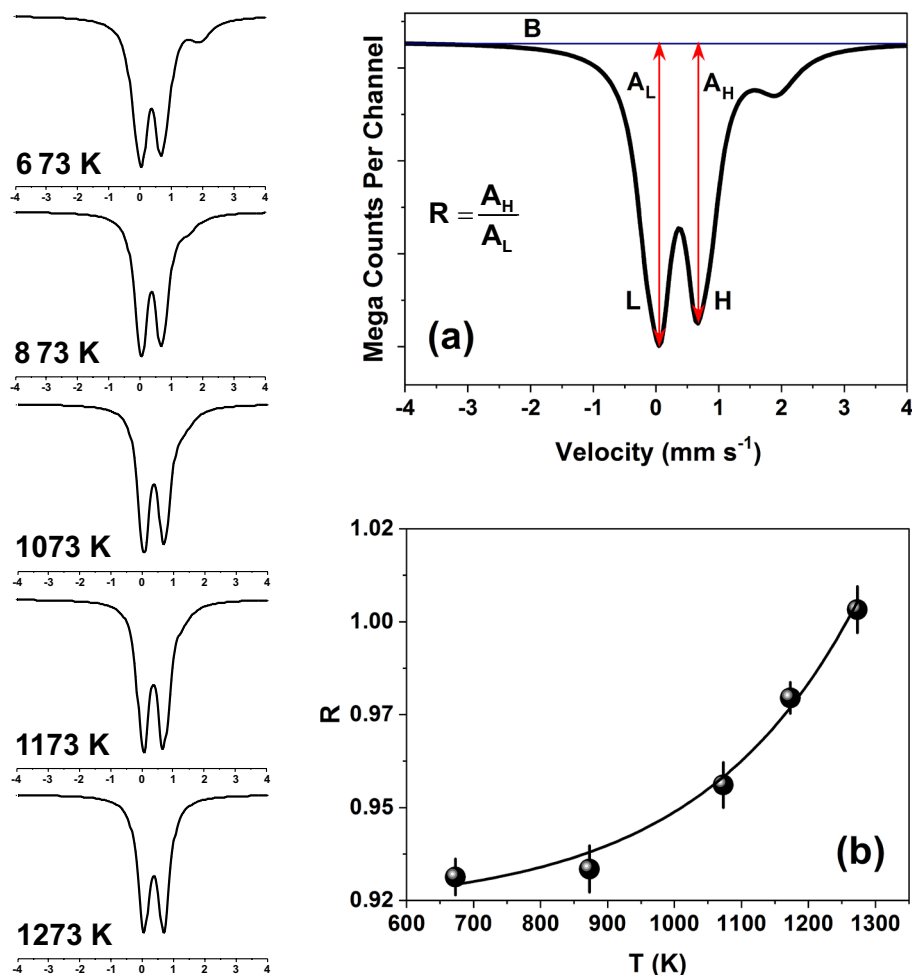


Fig. 4a – Explanation of the experimental parameter $R = A_H/A_L$ used in this work to describe changes of the two main absorption peaks in the Mössbauer spectra (left). B = value of off-resonance counting rate, L = low-energy peak, H = high-energy peak, A_L , A_H = amplitudes of these peaks. **b** – Variations in the parameter R with annealing temperature. Solid line represents the exponential regression: $R = R_0 + A \exp(b T)$ where $R_0 = 0.918(7)$, $A = 3.79(1) \times 10^{-4}$ and $b = 4.22(17) \times 10^{-3}$. Coefficient of determination $R^2 = 0.98$.

$$E_A = (0.45 \pm 0.02) \text{ eV} \quad (5)$$

The calculated activation energy of 0.45 eV for partially metamict davidite is significantly lower than those reported for track annealing in allanite (2.4 eV) (Saini et al. 1975), natural zircon (2.87 eV) (Virk 1995), $\text{CaZrTi}_2\text{O}_7$ doped with ^{244}Cm (5.8 eV), and synthetic zircon doped with ^{238}Pu (5.1–6.6 eV) (Weber et al. 1986; Weber 1991). It is also lower than the 1.97 eV value obtained in a similar way from Mössbauer spectroscopy for fully metamict gadolinite from Ytterby (Sweden) (Malczewski and Janeczek 2002). However, the value of 0.45 eV for partially metamict davidite is comparable to the value of 0.58 eV calculated for partially metamict gadolinite (Janeczek and Eby 1993). Values obtained after annealing of heavy ion tracks in micaceous minerals ranged from 0.63 eV (phlogopite) to 0.96 eV (muscovite) (Sandhu et al. 1987) (Tab. 2). Much lower activation energy was also reported for natural monazite irradiated by 800 keV Kr^{2+} ions (Meldrum et al. 1997).

The lower activation energy value measured for the davidite sample relative to those obtained for fully

metamict allanite, gadolinite and zircon reflects partial metamictization of the former. In a partially metamict state, crystalline domains coexist with smaller, irregular amorphous regions. This heterogeneity results in a lower activation energy measured during thermal recrystallization relative to that obtained for a completely metamict phase. In general, metamict oxides should have lower activation energy values than metamict silicates.

4. Conclusions

Based on ^{57}Fe Mössbauer spectroscopy, one stage of recrystallization was observed in a partially metamict davidite. Recrystallization in argon atmosphere occurred between 673 and 1273 K and was characterized by exponential growth in the ratio between amplitudes of the main absorption peaks and annealing temperature. A derivative function of the parameter relative to temperature was applied as a part of an isochronal annealing model to determine activation energy for thermally-induced recrystallization of examined davidite. Future research will

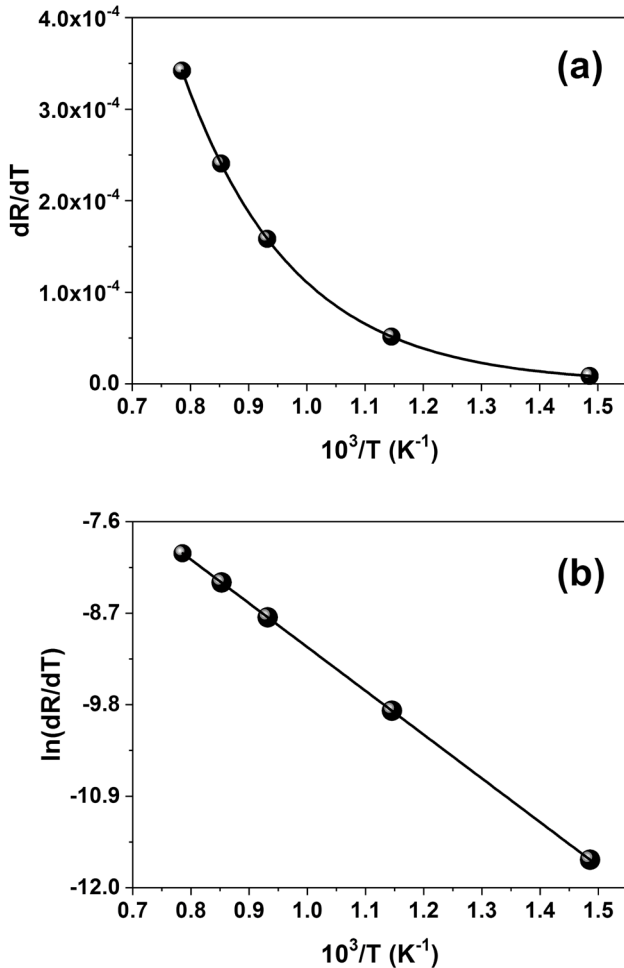


Fig. 5a – Plot of $\partial R/\partial T$ vs. T^{-1} . The solid line shows the exponential fit based on Eq. (2). **b** – Corresponding Arrhenius plot of $\ln(\partial R/\partial T)$ vs. T^{-1} . Solid line represents linear regression given by Eq. (3).

use the proposed isochronal annealing model to analyze other iron-bearing metamict phases using Mössbauer spectroscopy. The presence of Fe^{2+} in untreated, partially metamict davidite apparently results from Fe^{3+} to Fe^{2+} reduction in the radiation damage regions.

Acknowledgements. This work was supported by the National Science Centre of Poland grant no. 2018/29/B/ST10/01495. We thank reviewers for critical comments that improved the final version of this paper. The authors also thank Jakub Plášil and Vojtěch Janoušek for their help and editorial guidance.

References

BRANAGAN D (2007) Davidite and other early events in Australia's uranium story. *J Proc Roy Soc New South Wales* 140: 1–9
 GATEHOUSE BM, GREY IE, KELLY PR (1979) The crystal structure of davidite. *Amer Miner* 64: 1010–1017

HAWTHORNE FC (1988) Mössbauer spectroscopy. In: HAWTHORNE FC (ed) *Spectroscopic Methods in Mineralogy and Geology*. Mineralogical Society of America Reviews in Mineralogy 18: 255–340
 HAWTHORNE FC, GROAT LA, RAUSEPP M, BALL NA, KIMATA M, SPIKE FD, GABA R, HALDEN NM, LUMPKIN GR, EWING RC, GREGOR RB, LITTLE FW, ERCIT TS, ROSSMAN GR, WICKS FJ, RAMIK RA, SHERRIFF BL, FLEET ME, MCCAMMON C (1991) Alpha-decay damage in titanite. *Amer Miner* 76: 370–396
 JANECZEK J, EBY RK (1993) Annealing in radiation damage in allanite and gadolinite. *Phys Chem Miner* 19: 343–356
 LIMA DE FARIA J (1956) The standard thermal treatment in the identification of metamict minerals by X-ray powder patterns. *Bol Mus Lab Mineral Geol Fac Ciênc Univ Lisb* 7(24): 125–131
 LUMPKIN GR, BLACKFORD MG, COLELLA M (2013) Chemistry and radiation effects of davidite. *Amer Miner* 98: 275–278
 LUMPKIN GR, GAO Y, GIERÉ R, WILLIAMS CT, MARIANO AN, GEISLER T (2014) The role of Th–U minerals in assessing the performance of nuclear waste forms. *Mineral Mag* 78: 1071–1095
 MALCZEWSKI D (2010) Recrystallization in fully metamict gadolinite from Ytterby (Sweden), annealed in air and studied ^{57}Fe Mössbauer spectroscopy. *Amer Miner* 95: 463–471
 MALCZEWSKI D, DZIURÓWICZ M (2015) ^{222}Rn and ^{220}Rn emanations as a function of the absorbed alpha-doses from select metamict minerals. *Amer Miner* 100: 1378–1385
 MALCZEWSKI D, JANECZEK J (2002) Activation energy of annealed metamict gadolinite from ^{57}Fe Mössbauer spectroscopy. *Phys Chem Miner* 29: 226–232
 MALCZEWSKI D, MOLAK A (2011) Electrical properties of annealed, fully metamict $REE_2Fe^{2+}Be_2Si_2O_{10}$. *J Nucl Mater* 412: 239–249
 MALCZEWSKI D, DZIURÓWICZ M, KRZYKAWSKI T, GRABIAS A (2018) Spectroscopic characterization and thermal recrystallization study of an unknown metamict phase from Tuften quarry, southern Norway. *Canad Mineral* 56: 365–373
 MELDRUM A, BOATNER LA, EWING RC (1997) Displacive radiation effects in the monazite- and zircon-structure orthophosphates. *Phys Rev B* 56: 13805–13814
 MODGIL SK, VIRK HS (1985) Annealing of fission fragment tracks in inorganic solids. *Nucl Instrum Methods Phys Res B* 12: 212–218
 NEUMANN H, SVERDRUP TL (1960) Contributions to the mineralogy of Norway. No. 8. Davidite from Tuftan, Iveland. *Nor Geol Tidsskr* 40: 277–288
 ORLANDI P, PASERO M, ROTIROTI N, OLMI F, DEMARTIN F, MOËLO Y (2004) Gramaccioliite-(Y), a new mineral of the crichtonite group from Stura Valley, Piedmont, Italy. *Eur J Mineral* 16: 171–175

- PABST A (1961) X-ray crystallography of davidite. *Amer Miner* 46: 700–718
- PRIMAK W (1955) Kinetics of processes distributed in activation energy. *Phys Rev* 100: 1677–1689
- PRIMAK W (1960) Large temperature range annealing. *J Appl Phys* 31: 1524–1533
- ROUSE RC, PEACOR DR (1968) The relationship between senaite, magnetoplumbite and davidite. *Amer Miner* 53: 869–879
- SAINI HS, NAND L, NAGPAUL KK (1975) Annealing studies of fission tracks in allanite. *Contrib Mineral Petrol* 52: 143–145
- SANDHU SA, SINGH S, VIRK HS (1987) Annealing of fission fragment tracks in micaceous minerals. *Mineral J* 13: 254–259
- SEYDOUX-GUILLAUME AM, WIRTH R, NASDALA L, GOTTSCHALK M, MONTEL JM, HEINRICH W (2002) An XRD, TEM and Raman study of experimentally annealed natural monazite. *Phys Chem Miner* 29: 240–253
- SINGH Y, SAXENA A, BHATT AK, VISWANATHAN R, SHAJI TS, NANDA LK (2018) Crystallochemical studies on davidite from Bichun, Jaipur District, Rajasthan, India. *J Earth Syst Sci* 127: 1–14
- VIRK HS (1995) Single activation energy model of radiation damage in solid state nuclear track detectors. *Radiat Eff Defect Solids* 133: 87–95
- WEBER WJ (1991) Self-radiation damage and recovery in Pu-doped zircon. *Radiat Eff Defect Solids* 115: 341–349
- WEBER WJ, WALD JW, MATZKE HJ (1986) Effects of self-radiation damage in Cm-doped $Gd_2Ti_2O_7$ and $CaZrTi_2O_7$. *J Nucl Mater* 138: 196–209
- WHITTLE AWG (1959) The nature of davidite. *Econ Geol* 54: 64–81
- WÜLSER PA, BRUGGER J, MEISSER N (2004) The crichtonite group of minerals: a review of the classification. *Bull Soc Fr Minéral Cristallogr* 16: 76–77
- ZIETLOW P, BEIRAU T, MIHAILOVA B, GROAT LA, CHUDY T, SHELUG A, NAVROTSKY A, EWING RC, SCHLÜTER J, ŠKODA R, BISMAYER U (2017) Thermal annealing of natural, radiation-damaged pyrochlore. *Z Kristallogr* 232: 25–38